Effect of post-welding heat treatments on mechanical properties of double lap FSW joints in high strength aluminium alloys

E. Cerri
Dept. Innovation Engineering, University of Salento, Lecce (Italy)

ABSTRACT

The present study focuses on the effect of post-welding heat treatments on mechanical properties of double-lap Friction Stir Welded (FSW) joints in 2024T3 and 7075T6 aluminium alloys. Heat treatments were performed at aging and solution temperatures. Micro-hardness profiles measured on transversal sections of post-welded heat treated joints reveal conditions (temperature and time) of hardness homogeneity at top, bottom and central nugget zone along the whole measured profile. When hardness homogeneity is reached, fracture occurs in the nugget. The double lap FSW joints after post-welding heat treatments at low temperatures (200° and 300°C) have tensile properties comparable with the as-FSW joint and fracture occurs in 7075T6 Base Material. At higher temperatures, fracture strain is almost 50% of joints deformed after heat treatment at lower temperature and failure occurs inside the stir zone. Polarized Optical Microscopy (POM) and Scanning Electron Microscopy (SEM) analysis reveal a progressive change in grain size and morphology in high temperature post-welding heat treated joints, leading to Abnormal Grain Growth in the stir zone.

RIASSUNTO

Questo studio esamina l'effetto di trattamenti termici sulle caratteristiche meccaniche di giunti doppi sovrapposti ottenuti per FSW di leghe di alluminio 2024T3 e 7075T6. I trattamenti termici sono stati condotti a temperature prossime a quelle di solubilizzazione e a quelle tipiche dell'invecchiamento. I profili di micro durezza misurati sulle sezioni delle tre lamine sovrapposte evidenziano condizioni di omogeneità nei valori in funzione della temperatura e tempo di trattamento. Nei casi in cui ci sia omogeneità, la frattura avviene nel nugget del campione. I giunti trattati a 200° e 300°C hanno proprietà a trazione paragonabili a quelle del giunto non trattato e la rottura avviene nel materiale base della 7075T6. Dopo trattamento a temperature più alte, la duttilità si dimezza rispetto ai giunti trattati basse T e la frattura avviene nel nugget. Le osservazioni microstrutturali in microscopia ottica in luce polarizzata e al SEM rivelano una progressiva crescita dei grani con fenomeni di crescita abnorme.

KEYWORDS

FSW, aluminium alloys, post-welding heat treatment, mechanical properties.

INTRODUCTION

Friction Stir Welding (FSW) is a solid state joining method particularly suited for aluminium alloys, which are often difficult to be fusion welded without hot cracking, porosity or distortion. During welding, the material is frictionally heated to a temperature at which it becomes more plastic. The heat of friction and plastic flow arising from the rotating tool produce significant microstructural changes, which lead to local variations in the mechanical properties of the weld [1-5]. FSW is being targeted by the industry for structurally demanding applications to provide high-performance benefits [6]. The FSW zone consists of a weld nugget, a Thermomechanically Affected Zone (TMAZ) and a Heat Affected Zone (HAZ). From a microstructural point of view, the grain structure in the weld nugget is very fine and equiaxed causing a higher mechanical strength and ductility [7-12]. The very attractive mechanical properties are principally due to the strong grain refining effect of the process. The data available in literature demonstrated that the mean grain sizes resulting from the FSW process result at least 10 times smaller than those measured in the undeformed parent material [13-14]. Grain refinement is due to severe plastic deformation that occur during FSW [15].

Recently, some studies have been conducted on Friction Stir Welded joints after a heat treatment to evaluate the stability of the fine grain structure at high temperature. One interesting details is the presence of Abnormal Grain Growth (AGG) in the nugget. The occurrence of this phenomenon may be a problem if it leads to a decay of mechanical properties of the weld [16].

The aim of this work is to investigate the effect of post-welding heat treatments on mechanical properties of double-lap FSW joints in 2024T3 and 7075T6 aluminium alloys. A number of postwelding heat treatments on double-lap FSW joints have been performed at different temperatures and time, followed by tensile tests and micro-hardness measurements. Microstructure evolution was characterized by light microscopy and Scanning Electron Microscopy SEM. Abnormal Grain Growth (ABB) develops during post-welding heat treatments.

EXPERIMENTAL PROCEDURES

Sheets of aluminium alloys of different composition and thickness were friction stir lap welded using a tool travel speed of 80mm/min and a rotating speed of 1000 rpm. The chemical compositions of the 2024T3 and 7075T6 materials are given in Table 1. The configuration of the double lap joint is reported in fig. 1, showing 2024T3 with thickness of 1,3 mm and 7075T6 of 2 mm. The external sheets (2024T3) were welded parallel to the rolling direction while the central sheet (7075T6) was put in the long transverse direction for FSW process in order to limit potential effect of rolling texture. The weld parameters were optimised taking into account the mechanical properties of the softer alloy (7075T6).

The microstructure of the double lap joint was characterized by Light Microscopy and SEM in the base materials and in the weld nugget zone. Chemical etching was performed by Keller's reagent and anodization by a solution of 5% HBF_4 in methanol. Grains were observed by Polarized Optical Microscopy (POM) and statistical analysis performed on a population of 300 features. Tensile specimens, with a gauge length of 30 mm, a width of 10 mm were machined from the FSW sheets in order to have the loading axis normal to the welding direction. The tests were performed at room temperature and nominal strain rates of 10^{-3} and 10^{-4} s^{-1}.

Vickers micro hardness profiles were measured each 500 μm on the lateral polished surface and perpendicularly to weld nugget direction. The measurements were performed by a LEICA WMHT instrument using an indentation load of 500gf for a dwell time of 15 s.

Table 1. Chemical composition (% in weight) of the base materials

	Cu	Mg	Zn	Fe	Si	Mn	Cr	Ti	Al
7075T6	1.2÷2	2.1÷2.9	5.1÷6.1	≤0.5	≤0.4	≤0.3	0.18÷0.28	<0.2	rem
2024T3	3.8÷4.9	1.2÷1.8	≤0.25	≤0.5	≤0.5	0.3÷0.9	≤0.1	≤0.15	rem

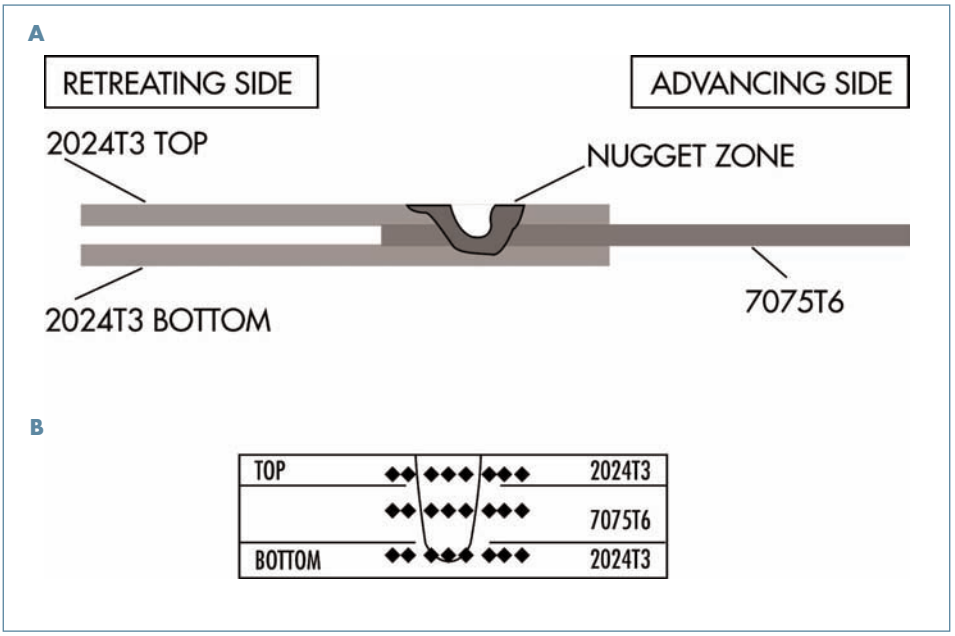

Fig. 1: a) Configuration of the double lap joint and b) scheme of the microhardness profiles

RESULTS AND DISCUSSION

WELD MICROSTRUCTURES AND PROPERTIES OF THE DOUBLE LAP FSW JOINT

The scheme of the double lap FSW joint is shown in Fig. 1a. The 2024T3 sheet at the top is called 2024T3 top, the 7075 T6 in the middle as 7075T6 and the 2024T3 on the bottom of the joints is identified as 2024T3 bottom. Fig. 1b illustrates microhardness profiles as measured on all the samples investigated.

The microstructure of the Base Materials (BM) and characteristic zones of the FSW double lap joint are shown in Fig. 2. Fig. 2a is a Polarized Optical Micrograph (POM) of the BMs showing the equiaxed grains of the 2024T3 top and bottom sheets with a mean size of 19,5 ± 0,5 μm, while the 7075T6 has elongated grains in the longitudinal direction. The equivalent grain diameter measured is 160 ±10 μm calculated by the intercept method. In the nugget (Fig. 2b), the grains are completely recrystallized with an equivalent dimension of 3,5±0,3 μm. The border between the TMAZ and the nugget (Fig. 2c) is easily defined because the severe plastic deformation has affected the morphology of the grains.

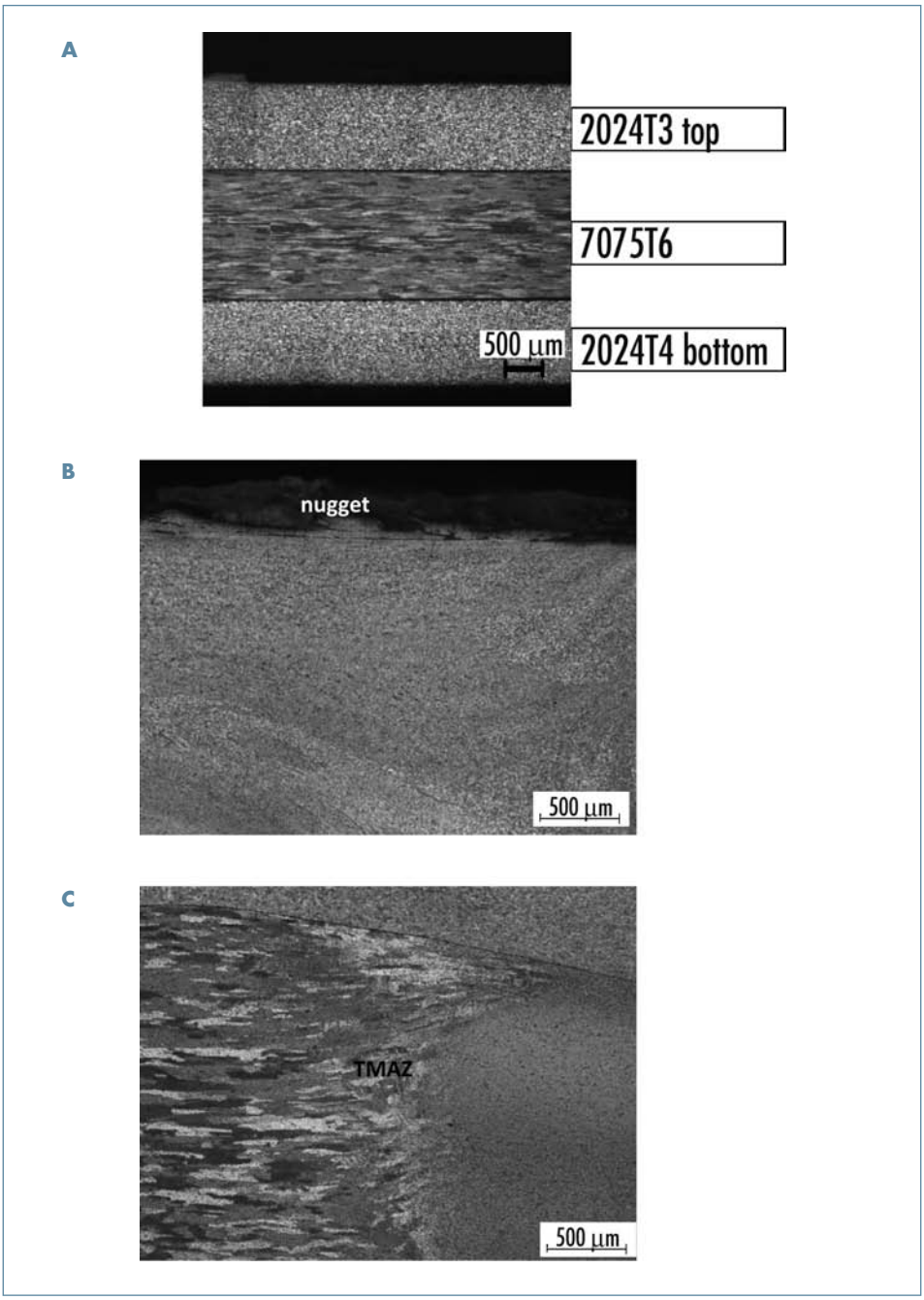

Fig. 2: Polarized light microscopy of double lap FSW joint. a) Base materials of 2024T3 top and bottom and 7075T6. b) nugget zone at the top and c) TMAZ and HAZ on the retreating side.

The interpretation of mechanical data depends also on particle type and not only on grain size. So it becomes of fundamental importance the study of particle type, their distribution in the different parts of the joint and the evolution during post-welding heat treatments. Fig. 3 shows particle distribution in the characteristic zones of the double lap joint. Particle distribution in the BMs are shown in Fig. 3a and 3b; in 2024T3 BM dispersoids and particles that spheroidized during homogenization are visible. Precipitates after T3 heat treatment are not resolved by optical microscopy. Fig. 3c and 3d illustrates particle distribution near the top of the double lap joint at the TMAZ and at the nugget center respectively, as indicated by circles in Fig. 3e. The border (TMAZnugget) is clearly distinguishable by changes in particle density and shape, as it occurs in Fig. 3f where TMAZ in correspondence of 7075T6-nugget is shown. In the nugget (Fig. 3d and 3g), particle density and distribution does not vary if the top and the center nugget are compared.

Particle identification has been performed by X-Rays diffractometry in the nugget and in the BMs on the plane parallel to the welding direction of double lap joint (fig. 4). The results show the presence of AlCuMg and AlFeSi type particles in the 2024T3 BM, of AlFeSi and $MgZn_2$ type particles in the 7075T6 BM and AlFeSi, AlCuMg and $MgZn_2$ in the nugget region. Even if in the nugget region all the different particle types are present, the peak heighs varied if compared to the BMs according to a different particle distribution in the nugget due to severe plastic deformation.

The variation in hardness profiles with distance from the weld centre has been measured along ideal lines of the three sheets as described in Fig. 1b, starting measurements from the BM through the nugget and to the opposite BM part. The results are plotted in Figs. 5-8. In the starting joint (fig. 5) the three micro-hardness profiles substantially differ in the stir zone and in the BMs, according to their thermal history and microstructure modifications occurred during severe plastic deformation of FSW. For the

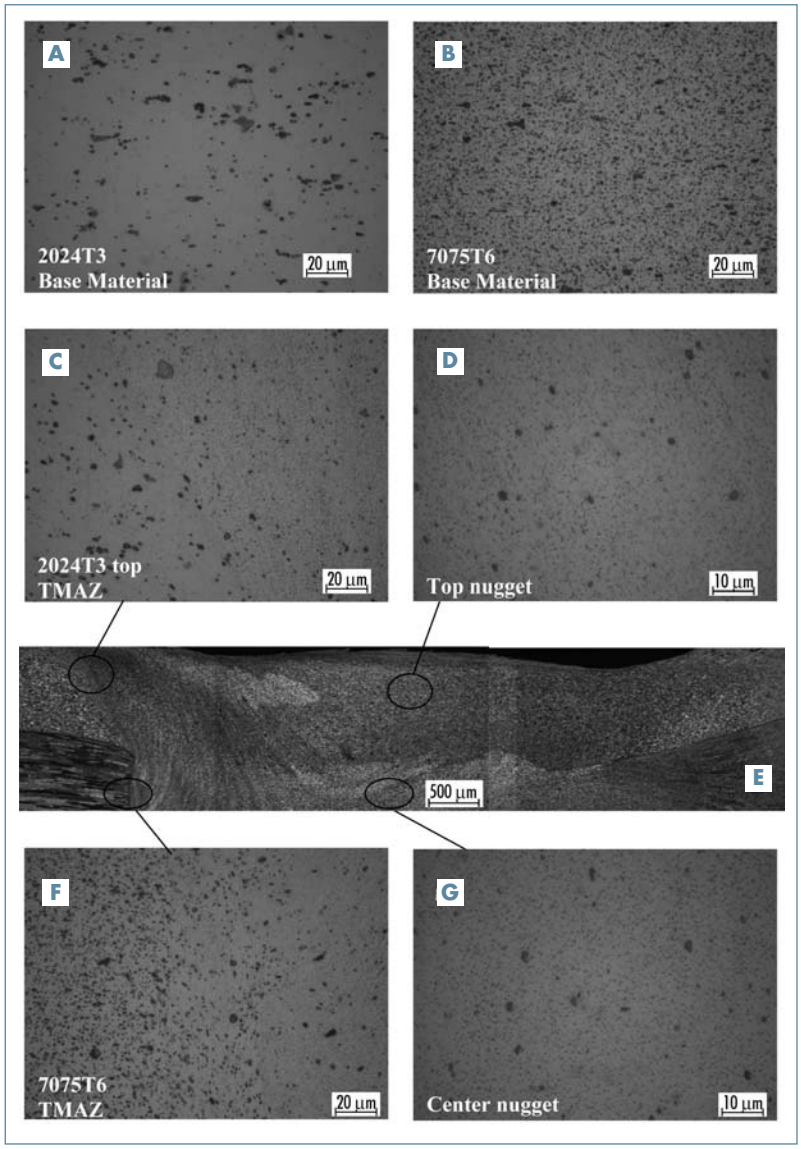

Fig. 3: Particle distribution after exposure at 200°C-1h in the double lap joint: a) 2024T3 and b) 7075T6 BMs; c) TMAZ in the 2024T3 top; d) top nugget; e) POM of the double joint; f) TMAZ at level of 7075T6; g) nugget center.

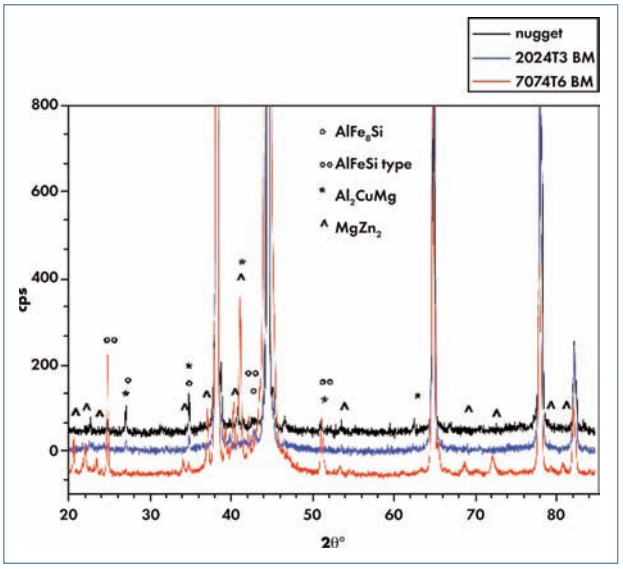

Fig. 4: X-Rays diffrattometry of the double-lap joint in the nugget and in the Base Materials showing particle identification.

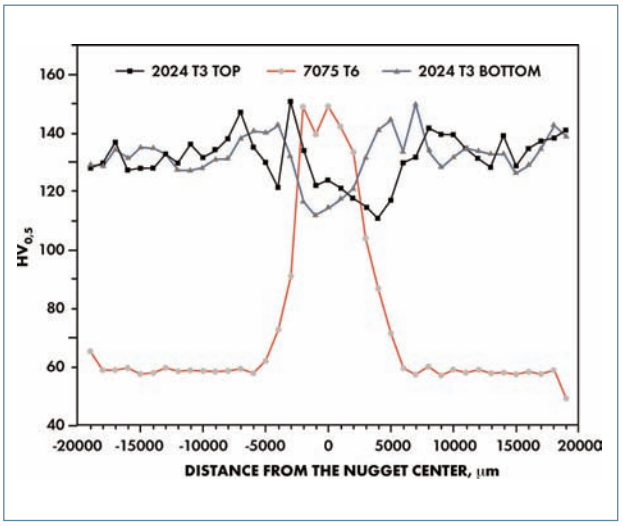

Fig. 5: Microhardness profile of as FSW double-lap joint.

2024T3 top and bottom Base Material, the hardness is in the range of 130-140 HV, then it increases in the TMAZ and reaching a minimum in the nugget region (110-120HV). In the 7075T6, the trend is reversed because hardness shows a maximum in the nugget zone (140-150 HV) and lower values in the BM (60HV). In order to explain this trend we should consider grain size and particle type and their distribution. The strong difference in grain shape and size of the two Base Materials is surely important. In fact, the 7075T6 BM presents the longitudinal plane perpendicular to the weld direction while the 2024T3 BM the transverse plane with an equivalent grain dimension that is 7-8 times larger in 7075T6 BM. This substantially contributes to the high difference in hardness of the BMs (7075T6 BM softer than 2014T3). Moreover, the central sheet is originally in T6 state while top and bottom are in T3 state. The particles (dispersoids or incoherent and stable) have been mostly revealed by X-rays diffractometry (fig. 4) but not precipitates. In the 2024T3 BM, TEM investigation performed by some of the authors in [17] showed the presence of submicron AlMnCu type particles but not very fine precipitates as expected. In the 7075T6 BM, other than AlCu and MgZnCu type particles, precipitates should be $Mg_{32}(Al,Zn)_{49}$ or $Mg(Zn_2,AlCu)$ or even $MgZn_2$ according to [18] of dimensions less than 100 nm. The T6 treatments has clearly provided recovery from the cold rolled condition without inducing recrystallization. The different precipitates, their distribution and grain size and state, let the 2024T3 BM to be much harder than 7075T6 BM (double).

In the stir zone or weld nugget, the hardness of the 2024T3 top and bottom lines is lower compared to the BM. At the same time, the hardness of the 7075T6 line (central line) in the nugget zone substantially increases to values comparable with 2024T3 BM. In the nugget, the central line has hardness values higher than in the top and bottom lines (fig.5). It is clear that FSW induces a strong grain refinement in the nugget (from 160 ±10 µm in

7075T6 BM to 3,5±0,3 μm) leading to a recrystallized state of the materials. Then, the difference in hardness between the centre and top-bottom regions of the nugget should depend on the capability of matrix solution strengthening. In fact during FSW, temperature increases over 400-450°C for aluminium alloys [19] and the solid solution condition is approached for both the alloys (solution T for 7075 is ≅ 470°C and for 2024 is ≅ 490°C). Moreover, the potential solute strengthening of the 7075 is high compared with the 2024 one and this strengthens the central zone of the nugget compared to the top and bottom. In Table 2, the tensile properties at room temperature of the double lap FSW joint and of the Base Materials are summarized. The double lap joint fractured in 7075T6 Base Material that has a higher UTS and lower ductility compared to 2024T3.

POST WELDING HEAT TREATMENTS

Double lap FSW joints have been heat treated at 200°, 300°, 400° and 450°C for time duration of 0.5-6h to study the thermal stability of microstructure and mechanical properties evolution.
Microstructure was evaluated by polarized

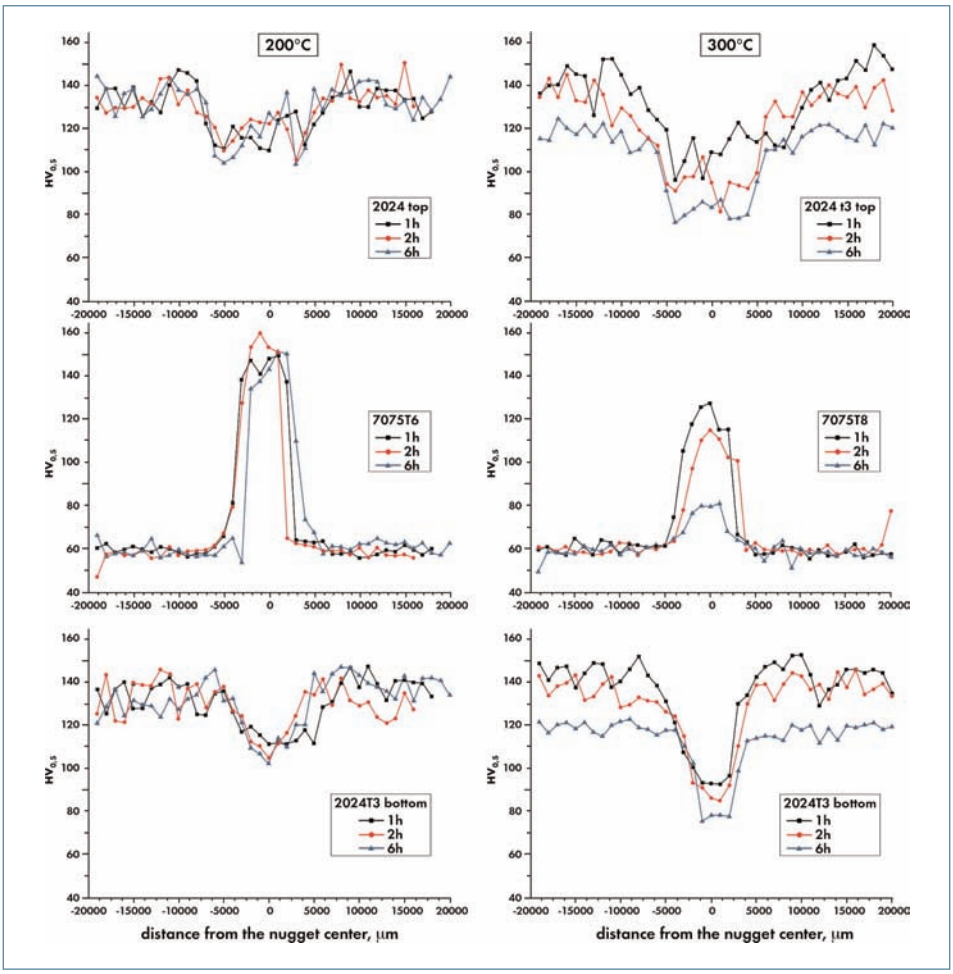

Fig. 6: Microhardness profiles measured after post-welding heat treatment at 200° (left side) and at 300°C (right side) as measured for the top, the center and the bottom line profiles.

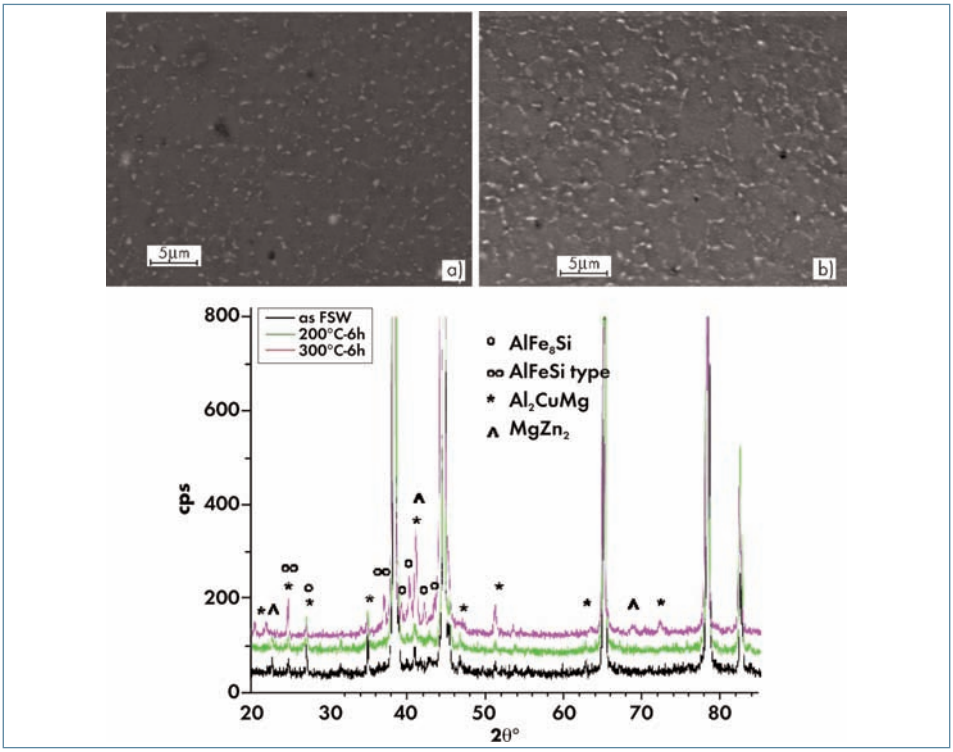

Fig. 7: Particle coarsening during exposure at 300°C for a) 2h and b) 6h. c) Comparison of X-Ray diffractometry of the as - FSW joint with joints exposed at 200° and 300°C for 6h.

light microscopy and SEM while mechanical properties by micro-hardness and tensile tests at room temperature. Fig. 6 illustrates micro-hardness profiles after exposure at 200° and 300°C for 1, 2 and 6h. The top microhardness profile is on the first row, the central microhardness profile on the central row and the bottom profile is on the third row. At 200°C (Fig. 6, left side), HV profiles are comparable with those of the FSW joint. A small increment of hardness in 2024T3 top (stir zone) delineates with time (after 6h). The exposure at 300°C (Fig. 6, right side) induces changes in hardness of the BMs and in the stir zones. In fact, the 2024T3 BM shows a decrease from 140-150 HV to 120 HV after 6h, while the 7075T6 BM remains constant. In the nugget, there is a progressive reduction in hardness for the 2024T3 and 7075T6 to comparable values (80-90 HV) in 6 hours. The decrease

of HV in 7075T6 nugget in 6 hours is very large (60 HV points). Moreover, micro-hardness profiles at 6 hours are less scattered compared with shorter time values. Fig. 7 reports BSE images of post-welded heat treated joints at 300°C for a) 2h and b) 6h showing particle distribution in the nugget zone. Particle size increases with time and their coarsening contributed

Table 2. Tensile properties of the FSW double lap joint and Base Materials

	Yield Strength, [MPa]	Ultimate Tensile Strength, [MPa]	Elongation, %
2024T3[19]	350	480	16
7075T6 [19]	530	600	8
FSW double lap joint	55	100	5

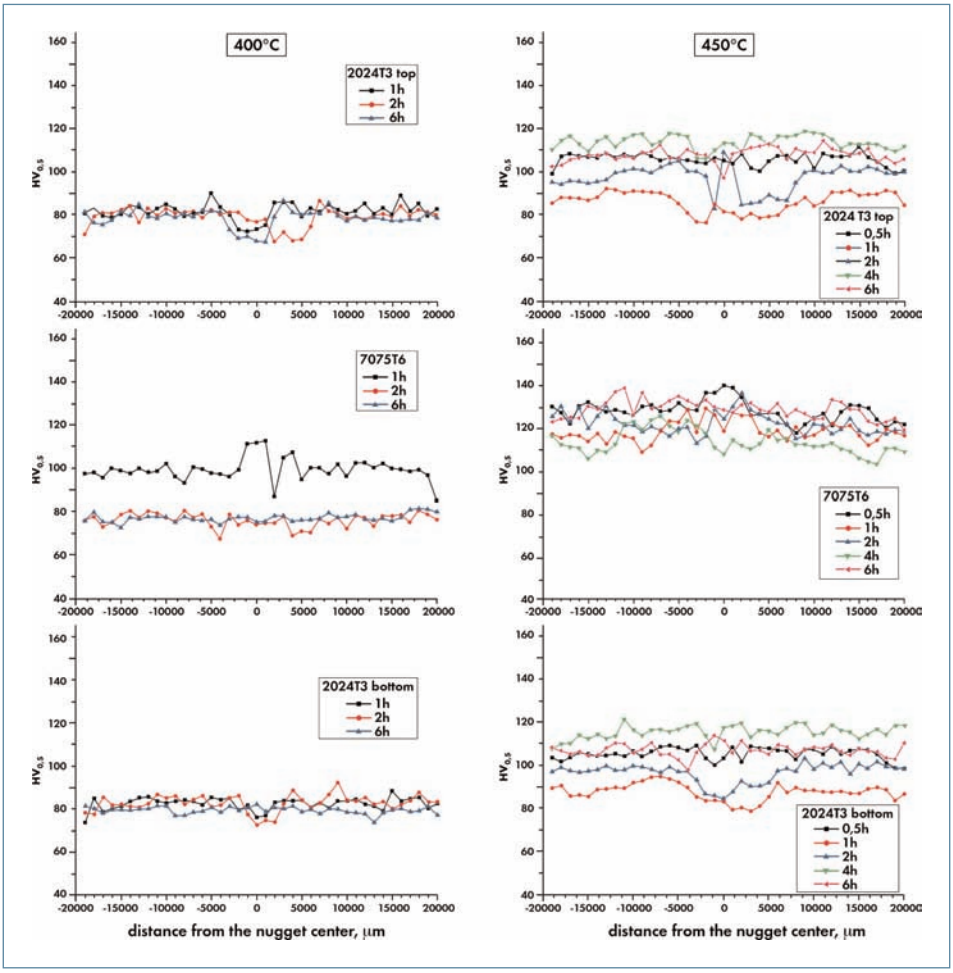

Fig. 8: Microhardness profiles measured after post-welding heat treatment at 400° (left side) and at 450°C (right side).

to lower HV profile in the nugget zone (fig. 7a,b). The evaluation of grain coarsening that may contribute to decrease hardness in the nugget with time has been shown in a recent paper [20]. X-Rays diffractometry performed in the nugget of 200°C-6h and 300°C-6h post-welded samples (fig. 7c) show an increase in peak intensity of Al_2CuMg and $MgZn_2$ compared to as FSW joint (nugget). This can be ascribed to coarsening of these particles that represent the most significative precipitation systems in 2024 and 7075 aluminium alloys respectively.

Fig. 8 illustrates micro-hardness measurements after post-welding heat treatments at high temperatures (400-450°C). After exposure at 400°C for 1h, HV profiles of the 2024T3 top and bottom are constant in the BMs (80 HV) and show a small minimum in the stir zone. The 7075T6 presents micro-hardness values around 100 HV in the BM and a large peak, 10 HV higher, in the stir zone. The difference between external and central section of the double lap joint is removed at 400°C-2h, even if the minimum still remains in the 2024T3 top. The double lap joint has reached homogeneity in hardness that is hold also at 400°C-6h.

Micro-hardness profiles have been measured after exposure at 450°C for 0.5, 1, 2, 4 and 6h (Fig. 8 on the right column). The HV profiles of 7075T6 remain similar in values (110-130HV) and shape at 450°C. The HV profiles of 2024T3 top and bottom tend to overlap and remain lower in values compared with those of the 7075T6. The joint and the whole nugget result homogeneous in hardness after 4h of post-welding treatment at 450°C. After this time, the HV profiles of the central 7075T6 and 2024T3 top and bottom are again separated. It is important to remark that HV profiles at 450°C-6h are almost constant, (i.e. few scattered points are present) although microstructure is very different in the nugget and in the BMs (AGG and elongated grains in 7075T6; AGG and transversal rolled grains in 2024T3 top and bottom) as it will be shown in the following. The microstructure of the nugget in the sample exposed at 400°C for 2h is shown in Fig.9. The grain size and shape are quite different in the 2024T3 and 7075T6 but the micro hardness values are comparable in the BMs. A strong contribution to levelling hardness comes from precipitation and/or dissolution processes occurring at 400°C in these alloys. The nugget still presents small equiaxed recrystallized grains.

During post-welding heat treatment at 450°C, the microstructure of the whole joint modifies, especially in the nugget zone (Fig. 9). In fact, after half an hour of exposure at 450°C, abnormal grains are visible at the bottom of the nugget zone. The extension of abnormal grains increases in volume with passing time and after four hours, abnormal grains occupy the whole nugget zone. The variation of microhardness at 450°C in the nugget zone can be due competing mechanisms occurring at 450°C: solid solution strengthening and over-ageing (very few) of particles. For the first hour the substantial softening in the nugget can be ascribed to

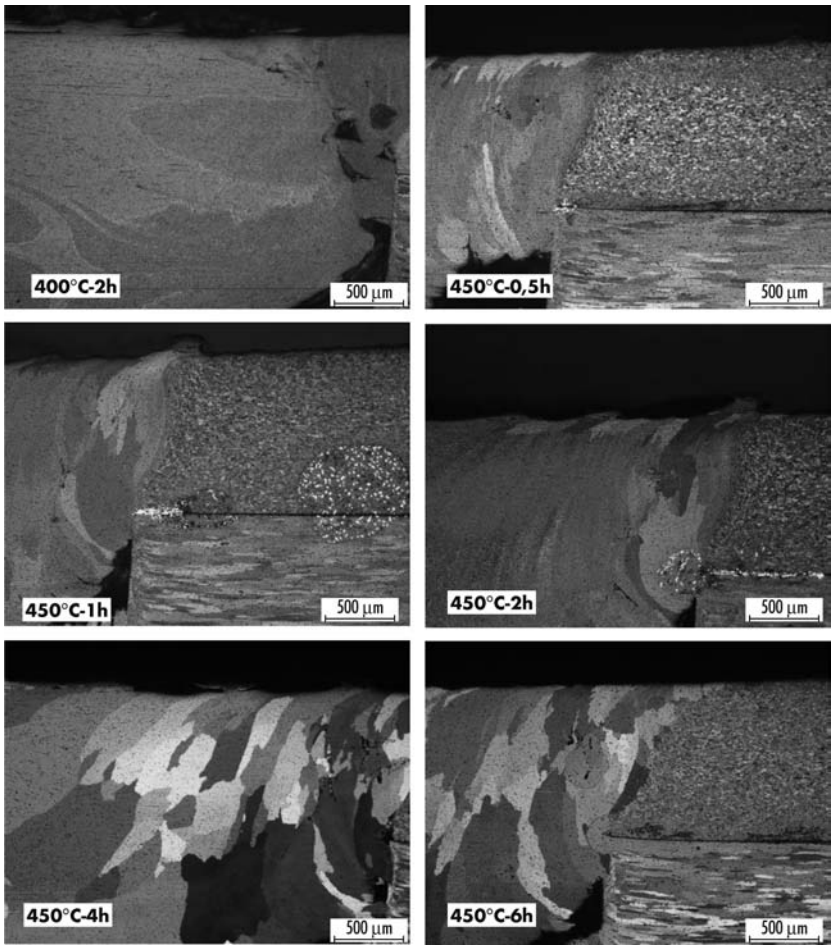

Fig. 9: Microstructure evolution at the nugget-TMAZ interface during exposure at high temperature.

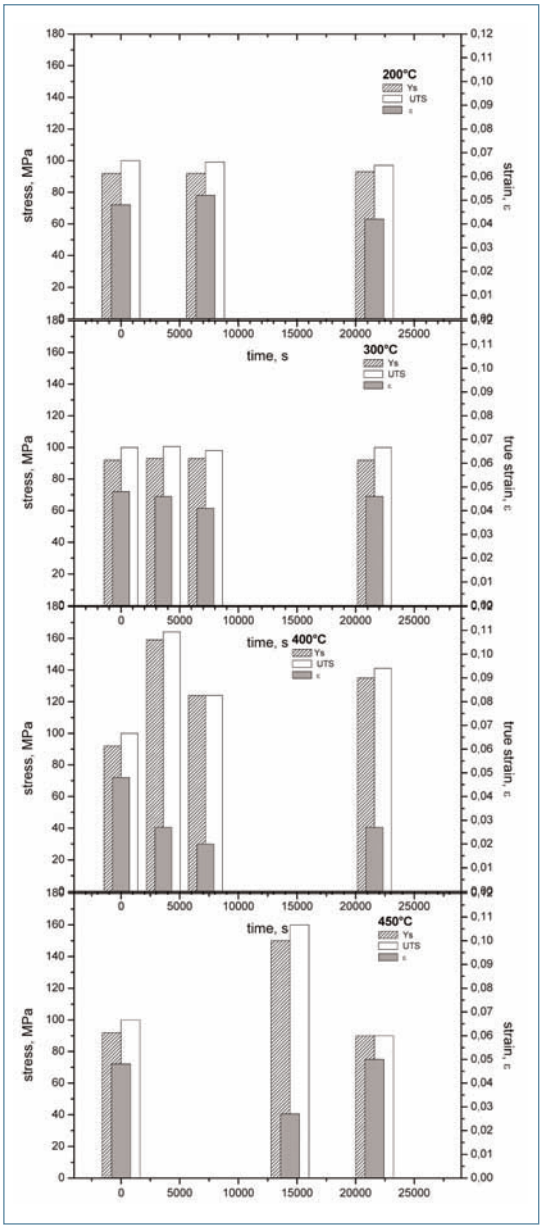

Fig. 10: Tensile properties after post-welding heat treatments vs. time of exposure.

over-ageing (solution temperature is close to 490°C) of a large quantity of S'/S particles. After 4 hour, a light softening due to overaging of equilibrium particles (S phase) [21,22] in shown in Fig. 8. For the 7075T6 nugget, the exposure at 450°C determines, at first, the complete dissolution of small particles and the coalescence of bigger ones giving rise to a light depression in microhardness values after 4 hours; afterwards, the solid solution strengthening mechanism increases again HV.

It is important to evaluate the effect of post welding-heat treatments on tensile properties of the double lap joints (Fig. 10). After low temperature heat treatments (200° and 300°C), the UTS are in the range of 90-100MPa and the elongations of 4-5%, quite far from the original sheet properties, as it results in Table 2. The fracture mode is also common for these joints because rupture occurs in the 7075T6 Base Material. Fracture of the joint was expected to occur in the 7075T6 BM because, according to HV profiles (Fig. 6), the post-welding heat treatments at 200° and 300°C do not substantially modify the initial HV profiles of the joints that were extremely inhomogeneous and let the 7075T6 BM be the softer part of the double lap joints.

The tensile behaviour of FSW joints after exposure at higher temperature (400° and 450°C) (Fig. 10) is different. Compared to lower heat treated joints, the stresses increase reaching an UTS of 160MPa for the sample post-welding heat treated at 400°C for 1h. The ductility remain rather low at 2-3%. In these samples, failure occurs inside the weld nugget and no more in the 7075T6 Base Material.

From micro-hardness profiles it was clear that the nugget zone was lightly softer than other regions of the joint, even for few hardness points.

The fracture location of post-welded FSW joints is shown in Fig. 11a. Actually in other samples, the fracture localized even in the 2024T3top. Fig. 11b is a low magnification SEM picture of the failure zone showing onion rings plastically deformed during tensile test. At higher magnifications (fig. 11c and d) fine microvoid distribution and particles are exhibited on the exposed abnormal grain surface.

CONCLUSIONS

Double lap Friction Stir Welded joints in 2024T3 and 7075T6 were subjected to post-welding heat treatments at aging and solution temperature and then to microhardness measurements and tensile test deformation at room temperature. The following conclusions were drawn from the results.

- The double lap FSW joints after post-welding heat treatment at low temperatures (200° and 300°C) have tensile properties comparable with the as-FSW joint one's. Also fracture occurs in the same region (7075T6 Base Material). At 300°C, microstructure evolution reduces hardness in the nugget and let hardness at the top, centre and bottom region to be comparable.
- Post-welding heat treatments at higher temperature (400° and 450°C) induces faster kinetics for particles coarsening and/or solubilisation and grain growth. At 400°C, micro-hardness profiles overlap after 2h, even if microstructure looks very different from BMs to nugget region. Fracture strain is almost 50% of joints deformed after heat treatment at lower temperature and failure occurs inside the stir zone. At 450°C, hardness profiles of the top, bottom and central line overlap after 4h exposure. At this time, Abnormal Grains occupy the whole nugget.

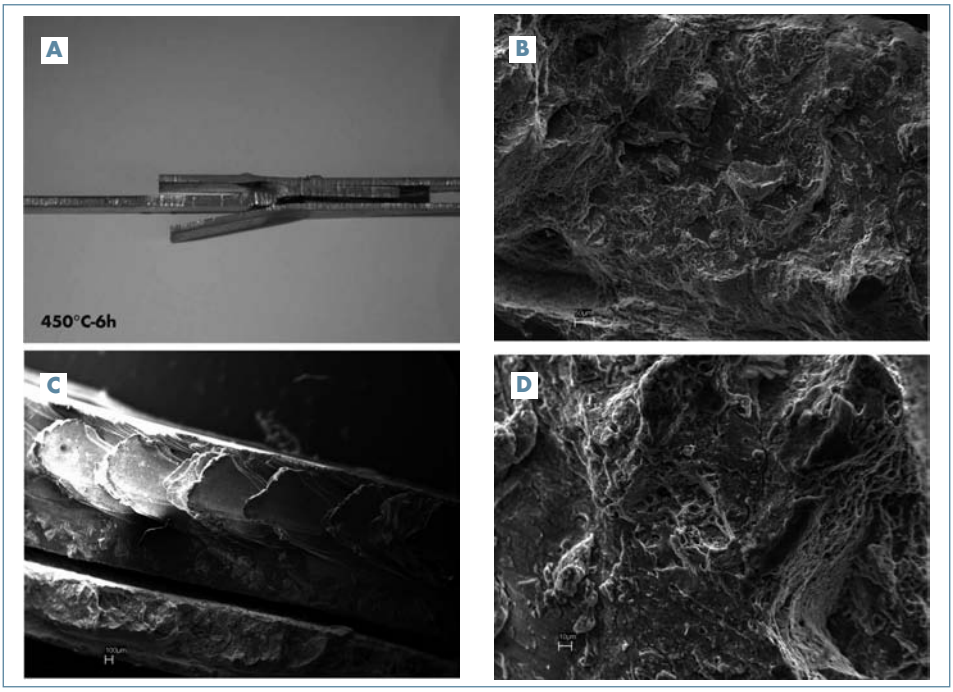

Fig. 11: Fracture zones in the double lap joint after exposure at 450°C-6h. a) low magnification picture showing the broken tensile sample; b) SEM picture of failure in correspondence of the 7075T6 central (nugget) showing extention of onion rings inside the nugget; c) and d) fracture surface at the centre and at the top of the nugget respectively.

ACKNOWLEDGEMENTS

The authors wish to thank MIUR for funding this research.

REFERENCES

[1] C.G. Rodes, M.W. Mahoney, W.H. Bingel, R.A. Spurling, C.C. Bampton. Effects of friction stir welding on microstructure of 7075 aluminum. Scripta Mater. 36 (1997) 69-75.

[2] M.W. Mahoney, C.G. Rodes, J.G. Flintoff, R.A. Spurling, W.H. Bingel. Properties of frictionstir- welded 7075 T651 Aluminum. Metall. Mater. Trans. A 29 (1998) 1955-1964.

[3] Y. Sato, H. Kokawa, M. Enomoto, S. Jogan. Microstructural evolution of 6063 aluminum during friction-stir welding. Metall. Mater. Trans. A 30 (1999) 2429-2437.

[4] K.V. Jata. Friction stir welding of high strength aluminium alloys. Mater. Sci. Forum 331-337 (2000) 1701-1712.

[5] R. Braun, C. Dalle Donne, G. Staniek. Laser beam welding and friction stir welding of 6013-T6 aluminium alloy sheet. Materialwissenschaft und Werkstofftechnik,. 31 (2000) 1017-1026.

[6] W.M. Thomas, E.D. Nicholas, J.C. Needam, M.G. Murch, P. Templesmith, C.J. Dawes, GB Patent application 9125978.8 (1991); 9125978.8, December 1991 and US Patent No. 5460317, October 1995.

[7] I. Charit, R. S. Mishra, M. W. Mahoney. Multi-sheet structures in 7475 aluminum by friction stir welding in concert with post-weld superplastic forming. Scripta Mater. 47 (2002) 631-636.

[8] H. G. Salem, A. P. Reynolds, J. S. Lyons. Microstructure and retention of superplasticity of friction stir welded superplastic 2095 sheet. Scripta Mater. 46 (2002) 337-342.

[9] C.G. Rhodes, M.W. Mahoney, W.H. Bingel, M. Calabrese. Fine-grain evolution in friction-stir processed 7050 aluminum. Scripta Mater. 48 (2003) 1451-1455

[10] K.V. Jata, S.L. Semiatin. Continuous dynamic recrystallization during friction stir welding of high strength aluminum alloys. Scripta Mater. (2000) 43 (8) 743-749.

[11] W. D. Lockwood, B. Tomaz, A.P. Reynolds. Mechanical response of friction stir welded AA2024: experiment and modelling. Mater. Sci. and Eng. A323 (2002) 348-353.

[12] M. Guerra, C. Schmidt, J.C. McClure, L.E. Murr, A.C. Nes. Flow Patterns during friction stir welding. Mat. Charac. 49 (2003) 95-101.

[13] G. Liu, L.E. Murr, C.S. Niou, J.C. McClure, F.R. Vega. Microstructural aspects of the frictionstir welding of 6061-T6 aluminum. Scripta Mater. 37 (1997) 355.

[14] L.E. Murr, G. Liu, J.C. McClur. Microtextures in the recrystallized zone of a friction-stir. J. Mater. Sci. Lett. 16 (1997)1801.

[15] P. Heurtier, C. Desrayaud, F. Montheillet. A Thermomechanical Analysis of the Friction Stir Welding Process. Mater Sci Forum 396-402 (2002) 1537.

[16] I. Charit, R.S. Mishra. Abnormal Grain Growth in Friction Stir Processed Alloys. Scripta Materialia 58 (2008) 367–371.

[17] E. Cerri, P. Leo, X. Wang and D. Embury, 'Mechanical properties and microstructure evolution of friction stir welded thin aluminium alloys', Metallurgical and Materials Trans. A, Volume 42, Issue 5 (2011), Page 1283-1295

[18] C.G.Rhodes, M. W. Mahoney, W.H.Bingel, R.A.Spurling, C.C. Bampton, Scripta Mater vol.36(1997) 69-75

[19] R.S. Mishra, Z.Y. Ma. Friction stir welding and processing. Mat. Sci. Eng. R 50 (2005) 1-78.

[20] E. Cerri, P. Leo, Mechanical properties evolution during post-welding heat treatments of double-lap Friction Stir Welded joints, Materials and Design (2011), in press.

[21] H. R. Shercliff, M.J. Russell, A. Taylor and T.L. Dickerson. Microstructural modelling in friction stir welding of 2000 series aluminium alloys. Mecanique & Industries 6, (2005) 25–35.

[22] M. Conserva, G. Donzelli, R. Trippodo, Aluminium and its applications, Edimet-Brescia (Italy) 1992.